

See discussions, stats, and author profiles for this publication at: <https://www.researchgate.net/publication/23284801>

Cyano Analogues of 7-Azaindole: Probing Excited-State Charge-Coupled Proton Transfer Reactions in Protic Solvents

ARTICLE *in* CHEMPHYSICHEM · OCTOBER 2008

Impact Factor: 3.42 · DOI: 10.1002/cphc.200800352 · Source: PubMed

CITATIONS

9

READS

33

8 AUTHORS, INCLUDING:



Kew-Yu Chen

Feng Chia University

66 PUBLICATIONS 822 CITATIONS

SEE PROFILE



Wan-Ting Hsieh

University of Pennsylvania

12 PUBLICATIONS 143 CITATIONS

SEE PROFILE



Chin-Hung Lai

Chung Shan Medical University

58 PUBLICATIONS 1,433 CITATIONS

SEE PROFILE



Jiun-Yi Shen

National Taiwan University

33 PUBLICATIONS 354 CITATIONS

SEE PROFILE

Cyano Analogues of 7-Azaindole: Probing Excited-State Charge-Coupled Proton Transfer Reactions in Protic Solvents

Cheng-Chih Hsieh, Kew-Yu Chen, Wan-Ting Hsieh, Chin-Hung Lai, Jiun-Yi Shen, Chang-Ming Jiang, Hsin-Sheng Duan, and Pi-Tai Chou^{*[a]}

The interplay between excited-state charge and proton transfer reactions in protic solvents is investigated in a series of 7-azaindole (7AI) derivatives: 3-cyano-7-azaindole (3CNAI), 5-cyano-7-azaindole (5CNAI), 3,5-dicyano-7-azaindole (3,5CNAI) and dicyanoethenyl-7-azaindole (DiCNAI). Similar to 7AI, 3CNAI and 3,5CNAI undergo methanol catalyzed excited-state double proton transfer (ESDPT), resulting in dual (normal and proton transfer) emission. Conversely, ESDPT is prohibited for 5CNAI and DiCNAI in methanol, as supported by a unique normal emission with high quantum efficiency. Instead, the normal emission undergoes prominent solvatochromism. Detailed relaxation dynamics and

temperature dependent studies are carried out. The results conclude that significant excited-state charge transfer (ESCT) takes place for both 5CNAI and DiCNAI. The charge-transfer specie possesses a different dipole moment from that of the proton-transfer tautomer species. Upon reaching the equilibrium polarization, there exists a solvent-polarity induced barrier during the proton-transfer tautomerization, and ESDPT is prohibited for 5CNAI and DiCNAI during the excited-state lifespan. The result is remarkably different from 7AI, which is also unique among most excited-state charge/proton transfer coupled systems studied to date.

1. Introduction

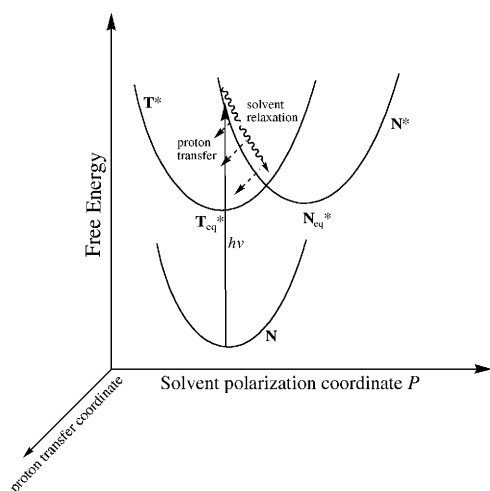
Due to its fundamental importance in chemical and biochemical reactions, the excited-state proton-transfer (ESPT) reaction has received much attention.^[1–2] One relevant, important area of current interest which is based on ESPT, is the coupled excited-state charge-transfer (ESCT) reaction. Theoretical approaches undertaken by Hynes and co-workers^[3] have described the key features of ESCT in terms of dynamics and electronic structure of the intermolecular proton-transfer reactions in protic solution. One of the questions raised is the nature of the quantum character of the proton in a proton transfer reaction. It has been revealed that the motion is always faster than the rearrangement of protic solvent molecules, and thus the Born-Oppenheimer approximation can be analogously made for the correlation between proton and solvent molecules in this reaction. As a consequence, the equilibrium between the moving proton and the surrounded solvent molecules is established at each instant, and the reaction activation free energy is thus essentially dominated by the solvent reorganization since charge redistribution is involved rather than the height of the proton migration barrier.

On this basis, various experimental approaches have been made and, according to the reaction pattern, can be categorized into two classes, namely the excited-state intermolecular proton transfer (i.e. deprotonation to the solvent pool) and intramolecular proton transfer. In view of excited-state intermolecular proton transfer, several elegant experiments have been performed and the results are well described by the aforementioned theoretical models.^[3,4] On the other hand, cases regarding intramolecular proton-transfer may ease the reaction complexity simply due to its unimolecular type of reaction (neg-

lecting the ion-pair forming process that involves the solvated proton and its counterpart). Technically, however, studies of proton/charge coupled reactions for the latter case cannot be facilitated without certain ingenious design of molecules possessing large dipolar changes between normal and proton transfer tautomers in the excited state.

However due to synthetic design of molecules, studies regarding solvent polarity influencing the excited-state intramolecular proton transfer have made significant progress.^[5–9] Many potential ESCT/ESPT systems have been designed and intensively investigated during the past few years to gain detailed insights into this fundamental issue. Prototypical examples include *para*-*N,N*-dialkylaminosalicylaldehyde^[5,7e], *N,N*-dialkylamino-3-hydroxy flavones,^[6–7] 2-hydroxy-4-(di-*p*-tolyl-amino)benzaldehyde^[8] and 2-(2'-hydroxy-4'-diethylaminophenyl)-benzothiazole,^[9] in which the *N,N*-dialkyl group is strategically designed to act as an electron donor (D), while the carbonyl oxygen or the nitrogen group within the parent ESPT moiety serves as an electron acceptor (A). Studies have concluded that most systems applied so far can be ascribed to an ultrafast (≤ 150 fs) ESCT prior to ESPT. Using *para*-*N,N*-dialkylaminosalicylaldehyde^[5,7e] as a model (see Scheme 1), the corresponding ESCT is an adiabatic type, that is, an optical electron-transfer

[a] C.-C. Hsieh, K.-Y. Chen, W.-T. Hsieh, Dr. C.-H. Lai, J.-Y. Shen, C.-M. Jiang, H.-S. Duan, Prof. P.-T. Chou
Department of Chemistry
National Taiwan University
No.1, Sec. 4, Roosevelt Rd., Da-an District, Taipei 106 (Taiwan)
Fax: (+886) 2-23695208
E-mail: chop@ntu.edu.tw

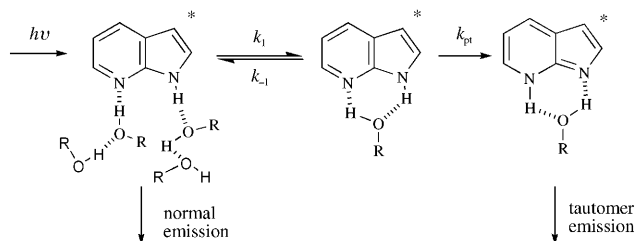


Scheme 1. The relaxation processes for a typical ESCT/ESPT system demonstrated by *para*-*N,N*-dialkylaminosalicylaldehyde in aprotic solvents.^[5,7e]

process. This can be rationalized by a strong π -electron overlap between donor and acceptor moieties, such that the electronic coupling matrix is much larger than that of the weak-coupling electron-transfer Marcus-type process.^[10] After reaching the solvent equilibration, due to the difference in equilibrium polarization between charge transfer (CT) and proton transfer (PT) species, the $CT^* \rightarrow PT^*$ (* denotes the electronically excited state) ESPT is associated with solvent induced barrier (see Scheme 1). Thus, despite a simple intramolecular type of ESPT, the results conclude the fundamental importance of the solvent polarity which plays a crucial role in the ESPT dynamics.

So far, the solvents applied to study charge-transfer coupled intramolecular proton transfer are all limited to aprotic molecules. It is thus of great fundamental interest to extend the concept toward protic solvents in view of potential biological applications. Unfortunately, in protic, hydrogen bonding solvents, the weakness or even rupture of the intramolecular hydrogen bond for the ESPT molecules results in a competitive deprotonation channel (to the bulk solvent), complicating the overall proton-transfer process.

From our viewpoint, ideal models to study the protic solvent effect on ESPT/ESCT reactions, are non-intramolecular hydrogen bonding molecules, in which the excited-state intramolecular proton transfer (if it occurs) must take place via solvent catalysis. As for probing ESPT in protic solvents, 7-azaindole (7AI, see Scheme 2) may serve as one of the most prominent



Scheme 2. The proposed ESPT mechanism in 7AI taken from ref. [12].

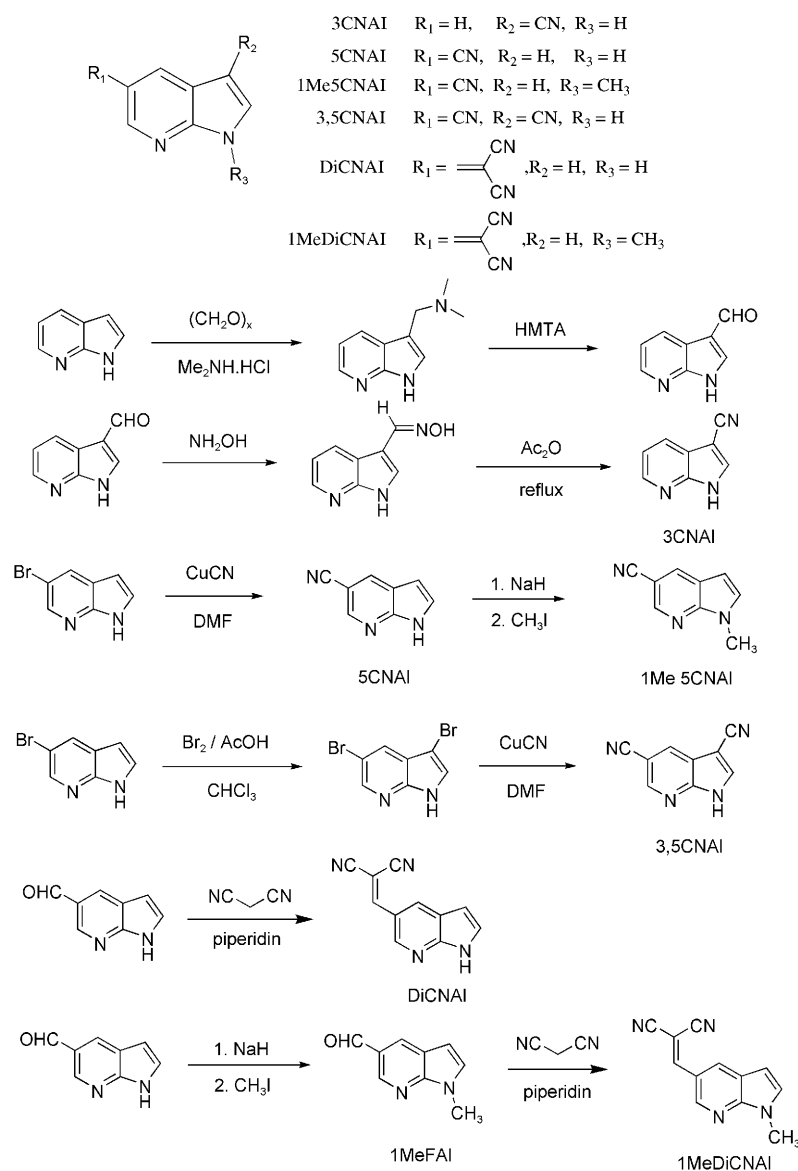
systems. 7AI possesses a unique photophysical property known as excited-state double proton transfer (ESDPT), which takes place either by solvent assistance (monomer in alcohols, see Scheme 2)^[11,12] or self-catalysis (dimer in nonpolar solvents),^[13] resulting in a proton-transfer tautomer emission. We thus propose to incorporate the electron donor/acceptor functionality into 7AI, such that charge transfer influencing ESPT can be investigated in protic solvents.

A series of 7AI derivatives, consisting of 3-cyano-7-azaindole (3CNAI),^[14] 5-cyano-7-azaindole (5CNAI), 3,5-dicyano-7-azaindole (3,5CNAI) and dicyanoethenyl-7-azaindole (DiCNAI) were synthesized (see Scheme 3). In this approach, the cyano functionalization serves as an electron withdrawing group, such that charge transfer may take place from the pyrrolic nitrogen to the cyano substituent. On the other hand, the pyrrolic hydrogen and the pyridinyl nitrogen act as proton donating and accepting groups, respectively (see Scheme 3). Due to the lack of intramolecular hydrogen bonds, proton transfer from pyrrolic hydrogen to pyridinyl nitrogen should take place in the presence of solvent molecules. The results and discussion elaborated in the following sections clearly demonstrate the role of protic solvent polarity in fine-tuning proton-transfer dynamics.

2. Results and Discussion

Figure 1 depicts the steady-state absorption and emission spectra of 3CNAI, 5CNAI, 3,5CNAI in methanol. Despite the similar absorption spectra observed among the three compounds, the corresponding emission character reveals differences. 3CNAI and 3,5CNAI exhibit dual emission in methanol, consisting of a short wavelength emission band maxima at 343 nm and 377 nm (the F_1 band), respectively, accompanied by a large Stokes shifted emission (the F_2 band) with a peak wavelength at 480 nm (3CNAI) and 515 nm (3,5CNAI). The similar excitation spectra for both bands, which are also identical with the absorption spectra, together with the concentration-independent dual emission (from 10^{-5} – 10^{-3} M), confirms that the dual emission originates from the same ground-state species. Accordingly, as established in the case of 7AI,^[11,12] the F_1 band is attributed to the normal emission (N^*), while the F_2 band originates from the proton-transfer tautomer emission (T^* , see Scheme 2). The precursor (N^*) \rightarrow successor (T^*) type of ESDPT is supported by a good correlation between the decay (rise) of the F_1 (F_2) band. For example, the decay time of the F_1 band for 3CNAI is 230 ± 30 ps, which, within experimental error, is identical with the rise time (240 ± 30 ps) of the F_2 band (see Table 1). Relatively slow proton transfer is resolved for 3,5CNAI. The rate of ESPT, taking an average of decay (690 ± 30 ps, F_1 band) and rise (710 ± 30 ps, F_2) components, is 1.43×10^9 s $^{-1}$ (700 ps) for 3,5CNAI (see Figure 2).

On the other hand, 5CNAI only exhibits a unique normal emission band maximized at 395 nm in methanol (see Figure 1). The unique 395 nm emission, together with the exceedingly long decay time of 4.8 ns and high quantum yield ($\Phi_f \sim 0.2$, see Table 1), lead us to conclude a lack of ESDPT for 5CNAI in methanol. The results are in sharp contrast to the



Scheme 3. Structures of various 7AI analogues. Synthetic routes of 5CNAI, 1Me5CNAI, 3,5CNAI, 3CNAI, DiCNAI, 1MeDiCNAI.

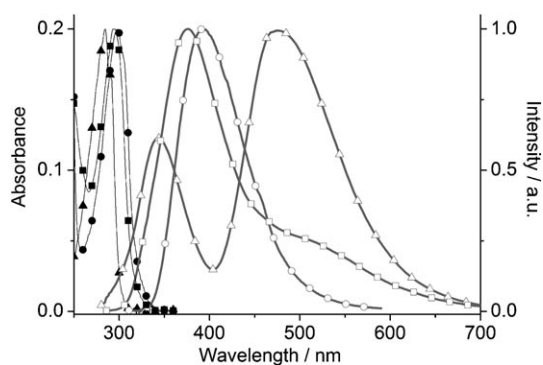


Figure 1. Absorption (black) and emission (gray) spectra of 3CNAI (–Δ–), 3,5CNAI (–□–) and 5CNAI (–○–) in methanol.

dual emission observed and hence the occurrence of ESDPT for both 3CNAI and 3,5CNAI. Accordingly, the relative CN (A) versus pyrrolic–NH (D) position seems to be crucial in describing the drastically different excited-state behavior. It has been well established that HOMO and LUMO of 7AI are largely resided at pyrrole and pyridine moieties, respectively.^[15] In view of the strong electron withdrawing property for the cyano group, upon electronic excitation, the occurrence of charge transfer in 5CNAI is expected via pyrrolic nitrogen to the cyano group.

To probe the ESCT state, the steady-state emission spectra of 5CNAI in various solvents are acquired (see Figure 3). Upon increasing the solvent polarity, despite the nearly solvent-independent absorption feature, the emission shows significant solvatochromism, being red-shifted from 329 nm in cyclohexane to 411 nm in water. In the controlled experiment, the same solvatochromic pattern is observed for 1Me5CNAI (see Figure 4), in which the hydrogen atom at N(1) is replaced by a methyl group, such that ESDPT is prohibited. Similar results between 5CNAI and 1Me5CNAI further support the lack of ESDPT in 5CNAI.

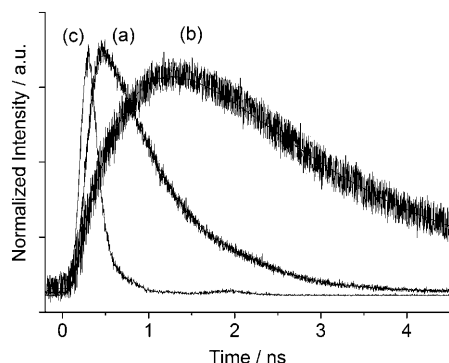
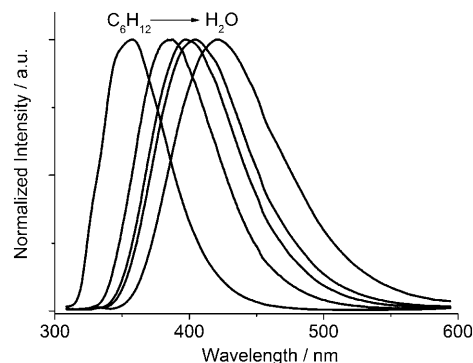
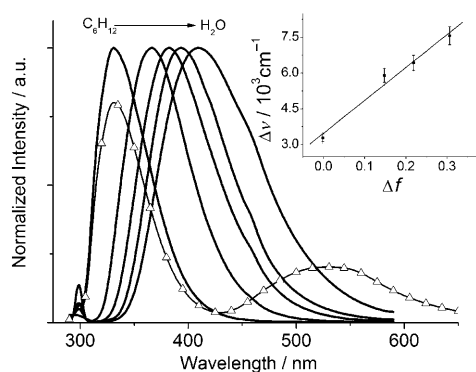
Applying a Lippert plot^[16] and estimating the radius of molecule a_0 to be 4.24 Å [Hartree–Fock theories with the 6-31++G(d',p') basis set, see Experimental Section], the change of dipole moment ($\Delta\mu = |\mu_e - \mu_g|$) between ground (μ_g) and excited (μ_e) states was deduced to be as large as 11.2 D for 5CNAI, supporting the proposed charge transfer properties. Relatively small solvatochromism is observed for 3CNAI (306–343 nm) and 3,5CNAI (323–377 nm) upon monitoring at the normal emission, and $\Delta\mu$ were deduced to be 7.4 D and 8.8 D for 3CNAI and 3,5CNAI, respectively. In comparison to 3CNAI, the larger dipolar change in 5CNAI can be rationalized by its longer D/A distance, while the partial cancellation between two push-pull dipole vectors in 3,5CNAI yields a net change of dipole moment in between 3CNAI and 5CNAI.

The tentative mechanism to rationalize the lack of ESDPT in 5CNAI, may imply that the great charge-transfer property of 5CNAI leads to a different distribution of the charge density

Table 1. Photophysical properties of 7AI, 3CNAl, 3,5CNAl, 5CNAl, and 1Me5CNAl in methanol.

	λ_{abs} [nm]	λ_{em} [nm] (Φ) ^[a]	τ [ns] ^[b]	$\Delta G^\ddagger + \Delta G^{+[\text{c}]}$ [kcal mol ⁻¹]
7AI ^[d]	288	374 503 (0.07)	τ : 0.146 τ_1 : 0.134 (−0.44) τ_2 : 0.654 (0.56)	2.07
3CNAl	285	343 480 (0.02)	τ : 0.23 τ_1 : 0.24 (−0.49) τ_2 : 5.88 (0.51)	2.22
3,5CNAl	294	377 515 (0.03)	τ : 0.69 τ_1 : 0.71 (−0.52) τ_2 : 1.13 (0.48)	2.63
5CNAl	297	395 (0.20)	τ : 4.8	
1Me5CNAl	301	404 (0.58)	τ : 19.2	
DiCNAl	351	600 (0.0014)	τ : 0.20	
1MeDiCNAl	359	587 (0.0016)	τ : 0.29	

[a] The reported Φ is the sum of the F_1 and F_2 bands. [b] Data in parentheses are the fitted preexponential factors. [c] Activation energy calculated from the temperature dependent decay time of fluorescence monitored at F_1 band. [d] Photophysical properties of 7AI are taken from ref. [11c, 12].

**Figure 2.** The relaxation dynamics of 3,5CNAl in methanol, monitored at a) 377 nm, b) 515 nm and c) the instrument response function.**Figure 4.** Emission spectra of 1Me5CNAl in cyclohexane, dichloromethane, acetonitrile, methanol, and water (from left to right).**Figure 3.** Emission spectra of 5CNAl in cyclohexane, dichloromethane, acetonitrile, methanol, and water (from left to right). (−Δ−): Emission of 5CNAl (10^{−5} M) in cyclohexane by adding 10^{−3} M methanol. Note in 10^{−5} M only normal emission was resolved without adding methanol. Inset: Lippert plot for 5CNAl in aprotic solvents (cyclohexane, chloroform, dichloromethane, and acetonitrile).

from that of 7AI, so that the driving force, for example, the basicity of pyridinyl nitrogen, for proton transfer is significantly reduced. However, this viewpoint seems contradictory to

5CNAl in cyclohexane titrated by trace of methanol, the results of which show a prominent methanol catalyzing double proton-transfer reaction, resulting in a proton-transfer tautomer emission with a maximum at 535 nm (see Figure 3).

As an alternative mechanism, since 5CNAl possesses a large $\Delta\mu$ value and hence greater solvent stabilization, one may propose that upon excitation and following fast solvent equilibrium, ESDPT of the solvated 5CNAl (denoted by 5CNAl_{eq}^{*}) is highly thermally unfavorable. To test this viewpoint, a computational

study (see Experimental Section) has been done. Upon treating methanol as the continuous solvent model, we calculated the normal species to be 17.22 kcal mol^{−1} lower in energy than the proton transfer tautomer in the ground-state. We then added the S_0 – S_1 gap by using the emission data, that is, 330 nm for normal species in methanol and 535 nm for the tautomer species (taken from the emission in cyclohexane titrated by methanol, see Figure 3) to the respective ground state. The results indicate that ESDPT in 5CNAl is thermally allowed by >2.2 kcal mol^{−1}.

We then made attempts to rationalize the results based on the widely accepted ESDPT mechanism for 7AI in protic solvents depicted in Scheme 2, in which the intrinsic proton-transfer rate constant $k_{\text{pt}} \ll k_{-1}$, such that the rate constant for an overall proton transfer process k_{ESPT} can be expressed by Equation (1)

$$k_{\text{ESPT}} = \frac{k_1}{k_{-1}} k_{\text{pt}} = k_{\text{pt}} e^{-\Delta G^\ddagger / RT} \quad (1)$$

in which ΔG^\ddagger is the difference in free energy between the cyclic and non-cyclic protic solvent solvated structure.^[12] The

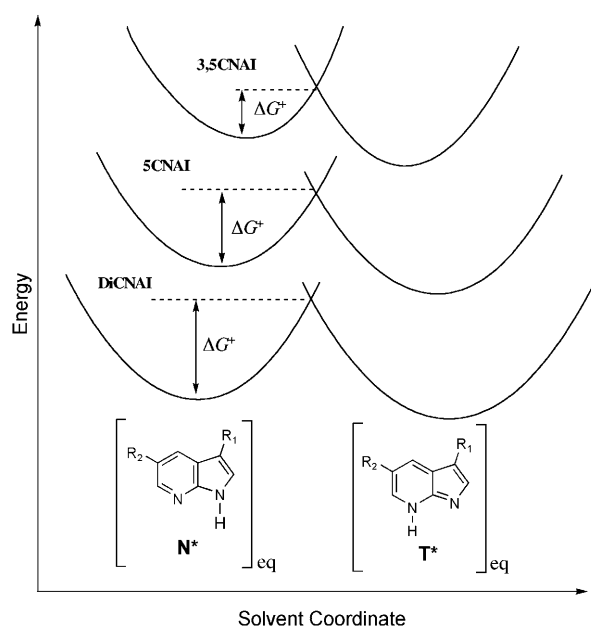
rather slow rate (~ 146 ps in methanol) of ESPT in 7AI is attributed to the equilibrium between the cyclic solvated structure and the non-cyclic solvated 7AI structure, in which only the cyclic solvated structure undergoes proton-transfer reaction. For the case of 7AI, ΔG^\ddagger value of $2.07 \text{ kcal mol}^{-1}$ is deduced.^[11c,12]

Assuming a similar k_{ptr} the difference in k_{ESPT} should lie in the difference of k_1/k_{-1} (i.e. ΔG^\ddagger). To gain more insight into the thermodynamics we have then made attempts to identify the energy difference by theoretical calculations. We first executed the geometry optimization of cyclic and non-cyclic structures for all the analogues based on HF/6-31++G(d',p'). The calculated energies of the non-cyclic forms minus the respective normal forms and two methanol molecules represent the free energy of formation of the non-cyclic form. A similar procedure is adopted for the cyclic form. The energetic value of the non-cyclic form is then subtracted from that of the cyclic form to obtain the free energy differences between the cyclic and non-cyclic structures. As a result, the ground-state energetic differences between the non-cyclic and cyclic forms are calculated to be 7.73, 7.45 and $7.61 \text{ kcal mol}^{-1}$ for 3CNAI, 5CNAI and 3,5CNAI, respectively. Such a difference, within the uncertainty of the calculation level, may be assumed to be negligible. This may be rationalized by the fact that the key chromophore, that is, 7AI, remains unchanged among the three analogues.

As for the excited state, it is believed that appreciably large uncertainty in energy may be introduced in the excited state using ab initio approaches. Nevertheless, it has been reported that the hydrogen-bonding structures for both cyclic and non-cyclic forms of 7AI do not differ much between the ground and excited states.^[12] We thus propose that a similar trend as that in the ground state—that is similar ΔG^\ddagger among 3CNAI, 5CNAI and 3,5CNAI—holds in the excited state. This approach is truly qualitative and simplified and its validity is pending further rigorous tests. Thus, under a similar k_{ptr} Equation (1) lacks a fundamental stance to rationalize the different k_1/k_{-1} (ΔG^\ddagger), particularly the prohibition of ESPT for 5CNAI in protic solvents.

We use a modified and more generalized reaction (Scheme 4) in an attempt to rationalize the experimental results of various 7AI analogues in this study. As depicted in Scheme 4, upon exciting the titled 7AI derivatives, ultrafast, adiabatic type ESCT takes place, followed by a fast ($< \text{few ps}$) solvent relaxation to reach the equilibrium polarization \mathbf{N}_{eq}^* . Due to its charge transfer character, it is reasonable to propose that the dipole moment of \mathbf{N}_{eq}^* is quite different from that of the proton transfer tautomer \mathbf{T}_{eq}^* in terms of magnitude and orientation, such that $\mathbf{N}_{\text{eq}}^* \rightarrow \mathbf{T}_{\text{eq}}^*$ is subject to a significant solvent-polarity perturbation.

To support this viewpoint, the dipole moments of \mathbf{N}^* and \mathbf{T}^* are calculated by TDDFT/B3LYP (see Experimental Section). For 5CNAI, the results estimate a dipolar vector of 10.95 D for \mathbf{N}^* , with an orientation of 171.9° relative to that of \mathbf{T}^* , for which the dipole moment was calculated to be 4.15 D (see Figure 5). The difference of dipole moment, $\Delta\mu$, between \mathbf{N}^* and \mathbf{T}^* was thus calculated to be as large as 15.07 D. As shown in Table 2, $\Delta\mu$, between \mathbf{N}^* and \mathbf{T}^* are calculated to be 5CNAI >



Scheme 4. The proposed mechanism of ESPT incorporating solvent polarity induced barrier in protic solvents following ESCT and solvent relaxation. Note that the subscript “eq” denotes the equilibrium polarization.

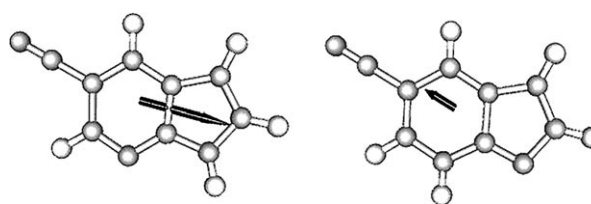


Figure 5. The orientations of the dipole moments of \mathbf{N}_{eq}^* (left) and \mathbf{T}_{eq}^* (right) of 5CNAI.

Table 2. The magnitudes (in Debye) and orientations of the dipole moments of \mathbf{N}^* and \mathbf{T}^* for 5CNAI, 3,5CNAI and 3CNAI, 7AI.

	$\mu(\mathbf{N}^*)$	$\mu(\mathbf{T}^*)$	$\Delta\mu$	$\theta[\mu(\mathbf{N}^*)-\mu(\mathbf{T}^*)]$
7AI	5.54	0.69	6.16	151.9°
3CNAI	4.07	3.90	5.87	94.84°
3,5CNAI	9.89	5.14	6.99	42.16°
5CNAI	10.95	4.15	15.07	171.9°
DiCNAI	19.28	12.51	31.47	163.2°

3,5CNAI > 3CNAI \sim 7AI. Although the calculated $\Delta\mu$ are somewhat different from that obtained from experimental results, qualitatively, the net result is consistent with a trend of the rate of ESPT being 7AI > 3CNAI > 3,5CNAI \gg 5CNAI (see Table 1). Although the level and method used in the current theoretical approach, to a certain extent, is not high enough for us to ensure the quantitative values, the results firmly support the correlation of changes of dipole moments between normal (\mathbf{N}_{eq}^*) and tautomer (\mathbf{T}_{eq}^*) species with respect to the observed ESPT dynamics. Note that this revised ESPT mechanism—which thermally incorporates the solvent-polarity induced barrier (into the experimentally derived ΔG^\ddagger) to reach a polariza-

tion configuration, in which \mathbf{N}^* and \mathbf{T}^* are energetically equal, that is, are in resonance for proton transfer/tunnelling (k_{pt})—essentially utilizes the same kinetic expression as Equation (1).

In the previous work of Hynes and co-workers, theoretical approaches for proton-transfer reaction in polar solvent have been carried out.^[3,17] Their results indicate that if the proton motion is treated in a quantum mechanic way, the timescale of proton vibration between proton donor and acceptor is comparably small to the timescale of rearrangement of surrounding solvent molecules. Solvent coordinate, rather than proton coordinate, should be viewed as the reaction coordinate. In the case of the 7AI analogues, the reaction barrier is mainly composed of solvent reorganization energy, which results from the difference in dipole moment in the proton-transfer process, that is, between \mathbf{N}_{eq}^* and \mathbf{T}_{eq}^* . Thus Equation (1) can be modified to Equation (2):

$$k_{\text{ESPT}} = \frac{k_1}{k_{-1}} k_{\text{pt}} = e^{-\Delta G^\ddagger / RT} \left[\frac{C_{00}^2}{h} \sqrt{\frac{\pi}{E_s RT}} e^{-\Delta G^\ddagger / RT} \right] \quad (2)$$

$$= \frac{C_{00}^2}{h} \sqrt{\frac{\pi}{E_s RT}} e^{-(\Delta G^\ddagger + \Delta G^\ddagger) / RT}$$

where C_{00}^2 represents the proton couplings' quantum average over the vibrational modes associated with the proton motion, E_s is the solvent reorganization free energy, and ΔG^\ddagger denotes the solvent induced barrier. Accordingly, the activation free energy represents not only the free energy difference between cyclic and non-cyclic solvated structures [see Scheme 2 and Eq. (1)] but also the incorporation of the solvent induced barrier.

We further performed the temperature dependent rate of proton transfer for 3CNAI and 3,5CNAI in methanol (see Figure 6). As a result, the effective barrier (ΔG^\ddagger plus solvent induced barrier) is determined to be 2.22 and 2.63 kcal mol⁻¹ for 3CNAI and 3,5CNAI, respectively (see Table 1 and Figure 6). The results correlate well with the increase of $\Delta\mu$ between \mathbf{N}_{eq}^* and \mathbf{T}_{eq}^* (vide supra). As for 5CNAI, due to the much larger $\Delta\mu$ between \mathbf{N}_{eq}^* and \mathbf{T}_{eq}^* , there apparently exists a significantly larger solvent-polarity induced barrier than that of 3,5CNAI,

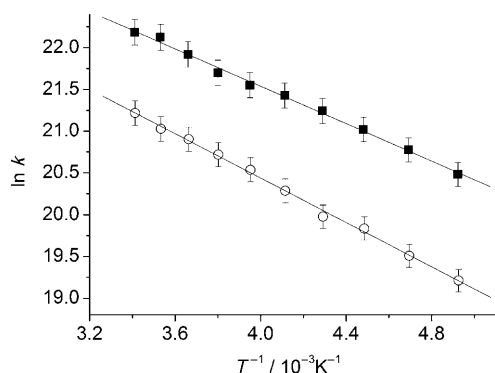


Figure 6. Temperature dependent time-correlated single photon counting experiment results of 3CNAI (■) and 3,5CNAI (○) in methanol. The linear relation between $\ln k$ and $1/T$ is shown, based on the Arrhenius equation.

3CNAI and 7AI, and thus proton transfer is too slow to compete with the rate of other excited-state deactivation process.

To further testify the above viewpoints, the molecule DiCNAI (see Scheme 3) was designed which has a much larger dipolar change during ESDPT. The absorption and emission spectra of DiCNAI recorded in various solvents are depicted in Figure 7A,

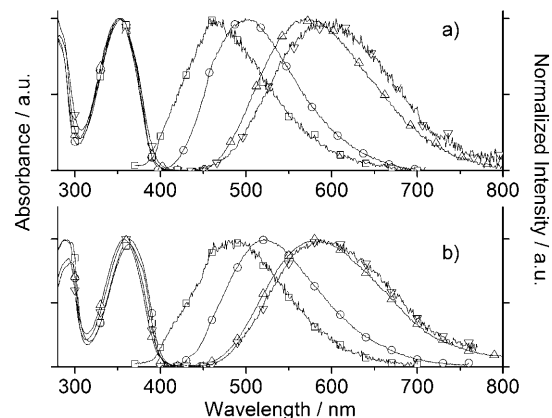


Figure 7. Absorption and emission spectra of a) DiCNAI and b) 1MeDiCNAI in benzene (—□—), dichloromethane (—○—), acetonitrile (—△—) and methanol (—▽—).

while the spectra for its methylated derivatives, that is, 1MeDiCNAI that represents non-proton transfer species are shown in Figure 7B. In comparison to the spectra of 1MeDiCNAI, there is no trace of tautomer emission for DiCNAI in methanol. Instead, significant solvatochromism takes place for both DiCNAI and 1MeDiCNAI, supporting the operation of a ESCT reaction. Based on the computation, the change of dipole moment, $\Delta\mu$, between \mathbf{N}^* and \mathbf{T}^* for DiCNAI is as large as 31D. Thus, similar to 5CNAI, we conclude the prohibition of ESDPT for DiCNAI in methanol due to the large effective barrier (ΔG^\ddagger plus solvent induced barrier ΔG^\ddagger). As for the ΔG^\ddagger , the results can be rationalized by an energy level versus solvent polarity diagram depicted in Scheme 4. As the dipole change associated with ESPT is increased, the two parabolas representing free energies for \mathbf{N}^* and \mathbf{T}^* , respectively, are increasingly separated along the solvent coordinate. We thus believe that an increase of the potential barrier for the 7AI analogues in polar solvent is due to a combination of the larger stabilization of the normal form and the greater separation of the solvent coordinates optimized for the normal and tautomer excited states. Thus, the trend of an increase of barrier is expected to be DiCNAI > 5CNAI > 3,5CNAI > 3CNAI.

3. Conclusions

Exploiting cyano derivatives of 7AI as prototypical models, we have demonstrated dipole-moment tuning ESCT/ESPT coupled reactions in protic solvents. For 5CNAI, the ESCT character in \mathbf{N}^* accounts for the large difference in dipole moments between \mathbf{N}_{eq}^* and \mathbf{T}_{eq}^* , resulting in the prohibition of ESPT. Conversely, the partial dipolar cancellation in 3,5CNAI makes ESPT

feasible. The trend of the observed ESPT dynamics are in good correlation with the proposed solvent-polarity induced barrier resulting from the difference in equilibrium polarization between N_{eq}^* and T_{eq}^* . This revised mechanism, although is based on a similar kinetic expression as Equation (1), intrinsically incorporates the solvent polarity effect and factors attributed to solute/solvent hydrogen bonding interaction such as solvent-induced barriers and possible energy differences between the cyclic and noncyclic solvated structures (see Scheme 2).^[12] At this stage, these two factors cannot be individually singled out. Furthermore, in the above approach [Eq. (2)], we simply assume that the solvent induced barrier for 7AI is negligible. This assumption, which is simply based on $\Delta\mu \sim 0$ between normal and tautomer species, could not be correct. Nevertheless, based on the above results, systematic investigation on ESCT/ESPT coupled reaction becomes possible in protic solvents, which may be crucial to gain fundamental insights into proton-coupled electron transfer in a living system. The results should spark a broad spectrum of interest in the field of proton-transfer reactions.

Experimental Section

Syntheses: Scheme 3 depicts synthetic routes of 5CNAI, 1Me5CNAI, 3CNAI, 3,5CNAI, DiCNAI, and 1MeDiCNAI. 3CNAI was synthesized according to the previous report.^[14] 5CNAI and 3,5CNAI were obtained via a modified procedure of a previous report. Briefly, cyanation of 5-bromo-7-azaindole by CuCN afforded 5CNAI. Subsequent *N*-alkylation of 5CNAI by methyl iodide gave 1Me5CNAI in good yield. In the synthesis of 3,5CNAI, the bromination of 5-bromo-7-azaindole, obtained 3,5-dibromo-7-azaindole, which subsequently underwent cyanation through a one-pot procedure to afford 3,5CNAI. Furthermore, DiCNAI and 1MeDiCNAI were synthesized via a piperidine catalyzed Knoevenagel reaction with manonitrile and 5-formyl-7-azaindole (purchased from Adesis) and 1MeFAI, respectively. 1MeFAI, was prepared by methylation of 5-formyl-7-azaindole. ¹H NMR and ¹³C NMR spectra were obtained with a Bruker AMX-400 spectrometer. Mass spectra (FAB) were recorded on a JMS-700 double focusing mass spectrometer (JEOL, Tokyo, Japan). 3CNAI was synthesized via the bromination of 7AI, followed by the cyanation to replace the bromo substituent. Detailed synthetic procedures and the corresponding structural characterization are elaborated as follows.

5CNAI: 5CNAI was synthesized via the reflux of a mixture of solution of 5-bromo-7-azaindole (100 mg, 0.51 mmol), cuprous cyanide (182 mg, 2.03 mmol), sodium iodide (76 mg, 0.51 mmol) and dry DMF (15 mL) for 48 h under nitrogen atmosphere. The reaction mixture was then poured into a 15 wt% aqueous ammonia solution. The yellow precipitate was filtered off, washed with ammonia solution and water, and vacuum dried. Further purification via column chromatography (hexane: ethyl acetate = 1:1) gave 5CNAI (43 mg, 60%). ¹H NMR (400 MHz, CDCl₃): δ = 9.48 (br, 1 H), 8.57 (s, 1 H), 8.24 (s, 1 H), 7.46 (d, *J* = 2.3 Hz, 1 H), 6.62 ppm (d, *J* = 2.3 Hz, 1 H). ¹³C NMR (100 MHz, CDCl₃): δ = 149.01, 145.92, 132.93, 127.16, 119.43, 118.54, 102.20, 101.59 ppm. MS (FAB): *m/z* (relative intensity) 143 (*M* + *H*⁺, 100), 116 (29). HRMS Calcd. for C₈H₅N₃ 143.0483. Found. 143.0480.

1Me5CNAI: 1Me5CNAI was synthesized via stirring a mixture of solution of 5CNAI (100 mg, 0.70 mmol), sodium hydride (97%, 100 mg, 4.00 mmol) and dry THF (10 mL) under nitrogen atmos-

phere at 0 °C for 30 min. Methyl iodide (150 mg, 0.11 mmol) was then added and the resulting mixture was stirred for 1 hour. The resulting mixture was diluted with 15 mL of water and extracted with CH₂Cl₂ (3 × 25 mL). Further purification via column chromatography (silica-gel column, hexane: ethyl acetate = 1:1) gave 1Me5CNAI (96 mg, 88%). ¹H NMR (400 MHz, CDCl₃): δ = 8.58 (d, *J* = 1.9 Hz, 1 H), 8.20 (d, *J* = 1.9 Hz, 1 H), 7.34 (d, *J* = 3.5 Hz, 1 H), 6.58 (d, *J* = 3.5 Hz, 1 H), 3.93 ppm (s, 3 H). ¹³C NMR (100 MHz, CDCl₃): δ = 148.27, 145.49, 132.65, 131.57, 119.68, 118.87, 100.70, 100.60, 31.45 ppm. MS (FAB): *m/z* (relative intensity) 157 (*M* + *H*⁺, 64), 156 (100). HRMS Calcd. for C₉H₇N₃ 157.0640. Found. 157.0636.

3,5CNAI: 3,5CNAI was prepared via refluxing a mixture of solution of 3,5-dibromo-7-azaindole^[18] (80 mg, 0.29 mmol), cuprous cyanide (208 mg, 2.32 mmol), sodium iodide (87 mg, 0.58 mmol) and dry DMF (25 mL) was refluxed for 72 h under nitrogen atmosphere. The reaction mixture was poured into a 15 wt% aqueous ammonia solution. The yellow precipitate was filtered off, washed with ammonia solution and water, and vacuum dried. Further purification via column chromatography (silica-gel column, hexane: ethyl acetate = 1:1) gave 3,5CNAI (7 mg, 14%). ¹H NMR (400 MHz, CD₃OD): δ = 8.69 (d, *J* = 1.8 Hz, 1 H), 8.55 (d, *J* = 1.8 Hz, 1 H), 8.33 ppm (s, 1 H). MS (FAB): *m/z* (relative intensity) 168 (*M* + *H*⁺, 100). HRMS Calcd. For C₉H₅N₄ 168.0436. Found. 168.0432.

DiCNAI: DiCNAI was synthesized via stirring a mixture of solution of 5-formyl-7-azaindole (146 mg, 1.00 mmol), malononitrile (330 mg, 5.00 mmol), a catalytic amount of piperidine, THF (10 mL) and MeOH (5 mL) at room temperature for 2 hour. The solution was extracted with ethyl acetate–water. Further purification via column chromatography (silica-gel column, dichloromethane: ethyl acetate = 1:1) gave DiCNAI (116 mg, 60%). ¹H NMR (400 MHz, CDCl₃): δ = 9.41 (br, 1 H), 8.82 (d, *J* = 1.9 Hz, 1 H), 8.56 (d, *J* = 2.0 Hz, 1 H), 7.86 (s, 1 H), 7.44 (d, *J* = 3.5 Hz, 1 H), 6.67 ppm (d, *J* = 3.5 Hz, 1 H). MS (FAB): *m/z* (relative intensity) 195 (*M* + *H*⁺, 10), 154 (100). HRMS Calcd. for C₁₁H₇N₄ 195.0669. Found 195.0671.

1MeFAI: 1MeFAI was synthesized via stirring a mixture of solution of 5-formyl-7-azaindole (102 mg, 0.70 mmol), sodium hydride (97%, 100 mg, 4.00 mmol) and dry THF (10 mL) under nitrogen atmosphere at 0 °C for 30 min. Methyl iodide (150 mg, 0.11 mmol) was then added and the resulting mixture was stirred for 1 hour. The resulting mixture was diluted with 15 mL of water and extracted with CH₂Cl₂ (3 × 25 mL). Further purification via column chromatography (silica-gel column, dichloromethane: ethyl acetate = 3:1) gave 1MeFAI (84 mg, 75%). ¹H NMR (400 MHz, CDCl₃): δ = 10.08 (s, 1 H), 8.79 (d, *J* = 1.8 Hz, 1 H), 8.36 (d, *J* = 1.8 Hz, 1 H), 7.25 (d, *J* = 3.5 Hz, 1 H), 6.58 (d, *J* = 3.5 Hz, 1 H), 3.90 ppm (s, 3 H). ¹³C NMR (100 MHz, CDCl₃): δ = 191.15, 150.19, 146.37, 131.23, 130.19, 125.30, 120.32, 101.61, 31.50 ppm. MS (FAB): *m/z* (relative intensity) 161 (*M* + *H*⁺, 100). HRMS Calcd. for C₉H₉O₂N₂ 161.0715. Found. 161.0714.

1MeDiCNAI: Using the procedure for DiCNAI, 1MeDiCNAI was prepared in 93% yield. ¹H NMR (400 MHz, CDCl₃): δ = 8.77 (d, *J* = 2.2 Hz, 1 H), 8.53 (d, *J* = 2.2 Hz, 1 H), 7.83 (s, 1 H), 7.29 (d, *J* = 3.6 Hz, 1 H), 6.61 (d, *J* = 3.6 Hz, 1 H), 3.90 ppm (s, 3 H). ¹³C NMR (100 MHz, CDCl₃): δ = 158.39, 149.72, 147.77, 132.19, 129.34, 120.84, 119.78, 114.22, 113.35, 102.06, 79.17, 31.58 ppm. MS (FAB): *m/z* (relative intensity) 209 (*M* + *H*⁺, 100). HRMS Calcd. for C₁₂H₉N₄ 209.0827. Found. 209.0829.

Measurements: Steady-state absorption and emission spectra were recorded by a Hitachi (U-3310) spectrophotometer and an Edinburgh (F5920) fluorimeter, respectively. The various solvents were of spectragrade quality (Merck Inc.) and were used right after being received. Dichloromethane and acetonitrile showed traces of

fluorescence impurities and were fractionally distilled prior to use. Detailed lifetime measurement has been described in the previous report.^[9,13e] Briefly, the fundamental pulses (750–840 nm) of a femtosecond Ti-Sapphire oscillator (80 MHz, Spectra Physics) was pulse-selected (Neos, model N17389) to reduce its repetition rate to typically 8–80 MHz, and then used to produce second harmonic (375–420 nm) and third harmonics (255–275 nm) as an excitation light source. Pico-nanosecond lifetime measurements were performed using a time-correlated single photon counting technique (Edinburgh OB 900L) as a detecting system. A polarizer was placed in the emission path to ensure that the polarization of the fluorescence was set at the magic angle (54.7°) with respect to that of the pump laser to eliminate the fluorescence anisotropy. The resolution of the time-correlated photon-counting system is limited by the detector response of ~50 ps. The fluorescence decays were analyzed by the sum of exponential functions with an iterative convolution method which allows partial removal of the instrument time broadening and consequently renders a temporal resolution of ~30 ps.

Theoretical Methodology: All calculations are done by Gaussian 03 program.^[19] The ground state geometries were optimized by HF/6-31++G(d', p').^[20] The radius of molecules estimated by this method are 4.24, 4.59, 4.14 Å for 5CNAl, 3,5CNAl, and 3CNAl, respectively. The dipole moments of **N*** and **T*** are calculated by TDDFT/B3LYP//HF/6-31++G(d', p') and a finite field strategy (0.001 au for the field factor) according to Hellmann-Feynman theory.

Acknowledgements

We thank National Science Council (grant numbers 99-1989-2004) for the financial support. We are also grateful to the National Center for High-Performance Computing of Taiwan for allowing us generous amounts of computing time.

Keywords: 7-azaindole • charge-coupled proton transfer • protic solvents • solvatochromism • tautomerization

- [1] a) A. Müller, H. Ratajczak, W. Junge, E. Diemann, *Studies in Physical and Theoretical Chemistry: Electron and Proton Transfer in Chemistry and Biology*, Vol. 78, Elsevier, Amsterdam, **1992**; b) J. Waluk, *Conformational Analysis of Molecules in Excited States*, Wiley-VCH, Weinheim, **2000**; c) T. H. Elsaesser, H. J. Bakker, *Ultrafast Hydrogen Bonding Dynamics and Proton Transfer Processes in the Condensed Phase*, Springer, Heidelberg, **2002**.
- [2] a) S. Scheiner, *J. Phys. Chem. A* **2000**, *104*, 5898–5909; b) L. M. Tolbert, K. M. Solntsev, *Acc. Chem. Res.* **2002**, *35*, 19–27; c) J. Waluk, *Acc. Chem. Res.* **2003**, *36*, 832–838; d) C. Tanner, C. Manca, S. Leutwyler, *Science* **2003**, *302*, 1736–1739; e) C. C. Cheng, C. P. Chang, W. S. Yu, F. T. Hung, Y. I. Liu, G. R. Wu, P. T. Chou, *J. Phys. Chem. A* **2003**, *107*, 1459–1471; f) S. Lochbrunner, A. J. Wurzer, E. Riedle, *J. Phys. Chem. A* **2003**, *107*, 10580–10590; g) R. de Vivie-Riedle, V. De Waele, L. Kurtz, E. Riedle, *J. Phys. Chem. A* **2003**, *107*, 10591–10599; h) M. Lukeman, P. Wan, *J. Am. Chem. Soc.* **2003**, *125*, 1164–1165; i) M. J. Paterson, M. A. Robb, L. Blancafort, A. D. DeBellis, *J. Am. Chem. Soc.* **2004**, *126*, 2912–2922; j) O.-H. Kwon, D.-J. Jang, *J. Phys. Chem. B* **2005**, *109*, 20479–20484; k) H. Hosoi, H. Mizuno, A. Miyawaki, T. Tahara, *J. Phys. Chem. B* **2006**, *110*, 22853–22860; l) P. W. Wu, W. T. Hsieh, Y. M. Cheng, C. Y. Wei, P. T. Chou, *J. Am. Chem. Soc.* **2006**, *128*, 14426–14427; m) R. Gelabert, M. Moreno, J. M. Lluch, *J. Phys. Chem. A* **2006**, *110*, 1145–1151.
- [3] a) P. M. Kiefer, J. T. Hynes, *J. Phys. Chem. A* **2002**, *106*, 1834–1849; b) P. M. Kiefer, J. T. Hynes, *J. Phys. Chem. A* **2002**, *106*, 1850–1861; c) J. T. Hynes, T.-H. Tran-Thi, G. Granucci, *J. Photochem. Photobiol. A* **2002**, *154*, 3–11.
- [4] a) E. Pines, B.-Z. Magnus, M. J. Lang, G. R. Fleming, *Chem. Phys. Lett.* **1997**, *281*, 413–420; b) Q. Cui, M. Karplus, *J. Phys. Chem. B* **2002**, *106*, 7927–7947; c) C. P. Andrieux, J. Gamby, P. Hapiot, J. M. Saveant, *J. Am. Chem. Soc.* **2003**, *125*, 10119–10124.
- [5] a) D. Gormin, M. Kasha, *Chem. Phys. Lett.* **1988**, *153*, 574–576; b) J. Heldt, D. Gormin, M. Kasha, *Chem. Phys.* **1989**, *136*, 321–334.
- [6] a) P. T. Chou, M. L. Martinez, J. H. Clements, *J. Phys. Chem.* **1993**, *97*, 2618–2622; b) F. Parsapour, D. F. Kelley, *J. Phys. Chem.* **1996**, *100*, 2791–2798; c) V. V. Shynkar, Y. Mély, G. Duportail, E. Piémont, A. S. Klymchenko, A. P. Demchenko, *J. Phys. Chem. A* **2003**, *107*, 9522–9529; d) A. D. Roshal, J. A. Organero, A. Douhal, *Chem. Phys. Lett.* **2003**, *379*, 53–59; e) S. Ameer-Beg, S. M. Ormson, X. Poteau, R. G. Brown, P. Fogg, L. Bus-sotti, F. V. R. Neuwahl, *J. Phys. Chem. A* **2004**, *108*, 6938–6943; f) P. T. Chou, S. C. Pu, Y. M. Cheng, W. S. Yu, Y. C. Yu, F. T. Hung, W. P. Hu, *J. Phys. Chem. A* **2005**, *109*, 3777–3787.
- [7] a) P. T. Chou, M. L. Martinez, J. H. Clements, *Chem. Phys. Lett.* **1993**, *204*, 395–399; b) T. C. Swinney, D. F. Kelley, *J. Chem. Phys.* **1993**, *99*, 211–221; c) S. M. Ormson, R. G. Brown, F. Vollmer, W. Rettig, *J. Photochem. Photobiol. A* **1994**, *81*, 65–72; d) F. Parsapour, D. F. Kelley, *J. Phys. Chem.* **1996**, *100*, 2791–2798; e) P. T. Chou, C. H. Huang, S. C. Pu, Y. M. Cheng, Y. H. Liu, Y. Wang, C. T. Chen, *J. Phys. Chem. A* **2004**, *108*, 6452–6454; f) Y. M. Cheng, S. C. Pu, Y. C. Yu, P. T. Chou, C. H. Huang, C. T. Chen, T. H. Li, W. P. Hu, *J. Phys. Chem. A* **2005**, *109*, 11696–11706.
- [8] P. T. Chou, W. S. Yu, Y. M. Cheng, S. C. Pu, Y. C. Yu, Y. C. Lin, C. H. Huang, C. T. Chen, *J. Phys. Chem. A* **2004**, *108*, 6487–6498.
- [9] Y. M. Cheng, S. C. Pu, C. J. Hsu, C. H. Lai, P. T. Chou, *ChemPhysChem* **2006**, *7*, 1372–1381.
- [10] a) M. J. Shephard, M. N. Paddon-Row, K. D. Jordan, *Chem. Phys.* **1993**, *176*, 289–304; b) M. N. Paddon-Row, M. J. Shephard, *J. Am. Chem. Soc.* **1997**, *119*, 5355–5365; c) A. M. Napper, N. J. Head, A. M. Oliver, M. J. Shephard, M. N. Paddon-Row, I. Read, D. H. Waldeck, *J. Am. Chem. Soc.* **2002**, *124*, 10171–10181; d) C. H. Lai, E. Y. Li, K. Y. Chen, T. J. Chow, P. T. Chou, *J. Chem. Theory Comput.* **2006**, *2*, 1078–1084.
- [11] a) C. A. Taylor, M. A. El-Bayoumi, M. Kasha, *Proc. Natl. Acad. Sci. USA* **1969**, *63*, 253–260; b) M. Negrier, S. M. Bellefeuille, S. Whitham, J. W. Petrich, R. W. Thornburg, *J. Am. Chem. Soc.* **1990**, *112*, 7419–7421; c) M. Negrier, F. Gai, S. M. Bellefeuille, J. W. Petrich, *J. Phys. Chem.* **1991**, *95*, 8663–8670; d) P. T. Chou, M. L. Martinez, W. C. Cooper, D. McMorro, S. T. Collins, M. Kasha, *J. Phys. Chem.* **1992**, *96*, 5203–5205; e) Y. Chen, R. L. Rich, F. Gai, J. W. Petrich, *J. Phys. Chem.* **1993**, *97*, 1770–1780; f) M. Negrier, F. Gai, J. C. Lambry, J. L. Martin, J. W. Petrich, *J. Phys. Chem.* **1993**, *97*, 5046–5049; g) R. L. Rich, Y. Chen, D. Neven, M. Negrier, F. Gai, J. W. Petrich, *J. Phys. Chem.* **1993**, *97*, 1781–1788; h) Y. Chen, F. Gai, J. W. Petrich, *J. Am. Chem. Soc.* **1993**, *115*, 10158–10166; i) F. Gai, R. L. Rich, J. W. Petrich, *J. Am. Chem. Soc.* **1994**, *116*, 735–746; j) R. L. Schowen, *Angew. Chem.* **1997**, *109*, 1502–1506; *Angew. Chem. Int. Ed. Engl.* **1997**, *36*, 1434–1438; k) A. V. Smirnov, D. S. English, R. L. Rich, J. Lane, L. Teyton, A. W. Schwabacher, S. Luo, R. W. Thornburg, J. W. Petrich, *J. Phys. Chem. B* **1997**, *101*, 2758–2769; l) D. E. Folmer, E. S. Wisniewski, J. R. Stairs, Jr., A. W. Castleman, *J. Phys. Chem. A* **2000**, *104*, 10545–10549; m) P. T. Chou, *J. Chin. Chem. Soc.* **2001**, *48*, 651–682.
- [12] a) R. S. Moog, M. Maroncelli, *J. Phys. Chem.* **1991**, *95*, 10359–10369; b) C. F. Chapman, M. Maroncelli, *J. Phys. Chem.* **1992**, *96*, 8430–8441; c) S. Mente, M. Maroncelli, *J. Phys. Chem. A* **1998**, *102*, 3860–3876.
- [13] a) A. Douhal, S. K. Kim, A. H. Zewail, *Nature* **1995**, *378*, 260–263; b) S. Takeuchi, T. Tahara, *Chem. Phys. Lett.* **1997**, *277*, 340–346; c) S. Takeuchi, T. Tahara, *J. Phys. Chem. A* **1998**, *102*, 7740–7753; d) T. Fiebig, M. Chachivili, M. Manger, A. H. Zewail, A. Douhal, I. Garcia-Ochoa, A. de La Hoz Ayuso, *J. Phys. Chem. A* **1999**, *103*, 7419–7431; e) W. S. Yu, C. C. Cheng, C. P. Chang, G. R. Wu, C. H. Hsu, P. T. Chou, *J. Phys. Chem. A* **2002**, *106*, 8006–8012; f) J. Catalán, P. Pérez, J. C. del Valle, J. L. G. de Paz, M. Kasha, *Proc. Natl. Acad. Sci. USA* **2002**, *99*, 5793–5798; g) J. Catalán, P. Pérez, J. C. del Valle, J. L. G. de Paz, M. Kasha, *Proc. Natl. Acad. Sci. USA* **2002**, *99*, 5799–5803; h) J. Catalán, P. Pérez, J. C. del Valle, J. L. G. de Paz, M. Kasha, *Proc. Natl. Acad. Sci. USA* **2004**, *101*, 419–422; i) K. Sakota, C. Okabe, N. Nishi, H. Sekuya, *J. Phys. Chem. A* **2005**, *109*, 5245–5247; j) J. Catalán, C. Diaz, P. Perez, J. L. G. de Paz, *J. Phys. Chem. A* **2006**, *110*, 9116–9122; k) S. Takeuchi, T. Tahara, *Proc. Natl. Acad. Sci. USA* **2007**, *104*, 5285–5290; l) O. H. Kwon, A. H. Zewail, *Proc. Natl. Acad. Sci.*

- USA **2007**, 104, 8703–8708; m) W. T. Hsieh, C. C. Hsieh, C. H. Lai, Y. M. Cheng, M. L. Ho, K. K. Wang, G. H. Lee, P. T. Chou, *ChemPhysChem* **2008**, 9, 293–299.
- [14] a) M. M. Robison, B. L. Robison, *J. Am. Chem. Soc.* **1955**, 77, 457–460; b) M. M. Robison, B. L. Robison, *J. Am. Chem. Soc.* **1956**, 78, 1247–1251; c) P. T. Chou, W. S. Yu, C. Y. Wei, Y. M. Cheng, C. Y. Yang, *J. Am. Chem. Soc.* **2001**, 123, 3599–3600.
- [15] a) R. Brause, D. Krügler, M. Schmitt, K. Kleinermanns, *J. Chem. Phys.* **2005**, 123, 224311; b) D. M. Rogers, N. A. Besley, P. O'Shea, J. D. Hirst, *J. Phys. Chem. B* **2005**, 109, 23061–23069; c) C. Kang, J. T. Yi, D. W. Pratt, *Chem. Phys. Lett.* **2006**, 423, 7–12.
- [16] J. R. Lakowicz, *Principles of Fluorescence Spectroscopy*, 2nd ed., Kluwer, Dordrecht, **1999**, p. 188.
- [17] a) P. M. Kiefer, J. T. Hynes, *J. Phys. Chem. A* **2003**, 107, 9022–9039; b) P. M. Kiefer, J. T. Hynes, *J. Phys. Chem. A* **2004**, 108, 11793–11808; c) P. M. Kiefer, J. T. Hynes, *J. Phys. Chem. A* **2004**, 108, 11809–11818.
- [18] B. Hugon, B. Pfeiffer, P. Renard, M. Prudhomme, *Tetrahedron Lett.* **2003**, 44, 3927–3930.
- [19] Gaussian 03 (Revision C.04), M. J. Frisch et al., Gaussian, Inc., Wallingford, CT, **2004**.
- [20] a) J. A. Pople, R. K. Nesbet, *J. Chem. Phys.* **1954**, 22, 571–572; b) G. A. Petersson, A. Bennett, T. G. Tensfeldt, M. A. Al-Laham, W. A. Shirley, J. Mantzaris, *J. Chem. Phys.* **1988**, 89, 2193–2218.

Received: June 10, 2008

Revised: August 24, 2008

Published online on September 26, 2008